



1     **Modeling the impact of heterogeneous reactions of chlorine on**  
2                   **summertime nitrate formation in Beijing, China**

3     Xionghui Qiu<sup>1,2</sup>, Qi Ying<sup>3\*</sup>, Shuxiao Wang<sup>1,2\*</sup>, Lei Duan<sup>1,2</sup>, Jian Zhao<sup>4</sup>, Jia  
4       Xing<sup>1,2</sup>, Dian Ding<sup>1,2</sup>, Yele Sun<sup>4</sup>, Baoxian Liu<sup>5</sup>, Aijun Shi<sup>6</sup>, Xiao Yan<sup>6</sup>,  
5                   Qingcheng Xu<sup>1,2</sup>, Jiming Hao<sup>1,2</sup>

6     <sup>1</sup> State Key Joint Laboratory of Environmental Simulation and Pollution Control,  
7     School of Environment, Tsinghua University. Beijing 100084, China.

8     <sup>2</sup> State Environmental Protection Key Laboratory of Sources and Control of Air  
9     Pollution Complex, Beijing 100084, China

10    <sup>3</sup> Zachry Department of Civil Engineering, Texas A&M University, College Station  
11    Texas, United States.

12    <sup>4</sup> State Key Laboratory of Atmospheric Boundary Layer Physics and Atmospheric  
13    Chemistry, Institute of Atmospheric Physics, Chinese Academy of Sciences, Beijing  
14    100029, China

15    <sup>5</sup> Beijing Environmental Monitoring Center, Beijing 100048, China

16    <sup>6</sup> Beijing Municipal Research Institute of Environmental Protection, Beijing 100037,  
17    China

18    \*Corresponding author: [shxwang@tsinghua.edu.cn](mailto:shxwang@tsinghua.edu.cn) & [qying@civil.tamu.edu](mailto:qying@civil.tamu.edu)

19    Abstract:

20    Abstract:  
21    A comprehensive chlorine heterogeneous chemistry is incorporated into the  
22    Community Multiscale Air Quality (CMAQ) model to evaluate the impact of chlorine-  
23    related heterogeneous reaction on diurnal and nocturnal nitrate formation and quantify  
24    the nitrate formation from gas-to-particle partitioning of HNO<sub>3</sub> and from different  
25    heterogeneous pathways. The results show that these heterogeneous reactions increase  
26    the atmospheric Cl<sub>2</sub> and ClNO<sub>2</sub> level, leading to an increase of the nitrate concentration  
27    by ~10% in the daytime. However, these reactions also lead to a decrease the nocturnal  
28    nitrate by ~20%. Sensitivity analyses of uptake coefficients show that the empirical  
29    uptake coefficient for the O<sub>3</sub> heterogeneous reaction with chlorinated particles may lead

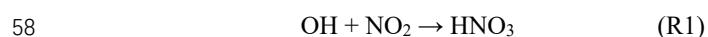


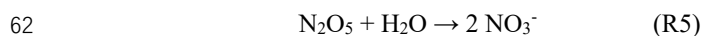
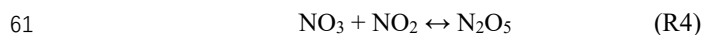
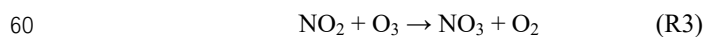
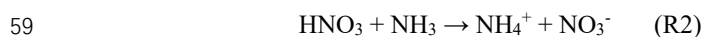
30 to the large uncertainties in the predicted Cl<sub>2</sub> and nitrate concentrations. The N<sub>2</sub>O<sub>5</sub>  
31 uptake coefficient with particulate Cl<sup>-</sup> concentration dependence performs better to  
32 capture the concentration of ClNO<sub>2</sub> and nocturnal nitrate concentration. The reaction  
33 rate of OH and NO<sub>2</sub> in daytime increases by ~15% when the heterogeneous chlorine  
34 chemistry is incorporated, resulting more nitrate formation from HNO<sub>3</sub> gas-to-particle  
35 partitioning. By contrast, the contribution of the heterogeneous reaction of N<sub>2</sub>O<sub>5</sub> to  
36 nitrate concentrations decreases by about 27% in the nighttime when its reactions with  
37 chlorinated particles are considered. However, the generated gas-phase ClNO<sub>2</sub> from the  
38 heterogeneous reaction of N<sub>2</sub>O<sub>5</sub> and chlorine-containing particles further decompose to  
39 increase the nitrate by 6%. In general, this study highlights the potential of significant  
40 underestimation of daytime and overestimation of nighttime nitrate concentrations for  
41 chemical transport models without proper chlorine chemistry in the gas and particle  
42 phases.

43

#### 44 **Introduction**

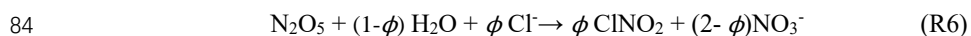
45 In recent years, nitrate has become the primary component of PM<sub>2.5</sub> (particulate matter  
46 with aerodynamic diameter less than 2.5 μm) in Beijing with sustained and rapid  
47 reduction of SO<sub>2</sub> and primary particulate matter emissions (Ma et al., 2018; Li et al.,  
48 2018; Wen et al., 2018). Observations showed that the relative contributions secondary  
49 nitrate in PM<sub>2.5</sub> could reach up to approximately 50% during some severe haze pollution  
50 days (Li et al., 2018). The mechanism of secondary nitrate formation can be  
51 summarized as two major pathways: (1) Gas-to-particle partitioning of HNO<sub>3</sub>, which  
52 happens mostly in the daytime. The reaction of OH with NO<sub>2</sub> produces gaseous HNO<sub>3</sub>,  
53 which subsequently partition into the particle phase. The existence of NH<sub>3</sub> or basic  
54 particles enhances this process by NH<sub>3</sub>-NH<sub>4</sub><sup>+</sup> gas-particle equilibrium; (2) Hydrolysis  
55 of N<sub>2</sub>O<sub>5</sub>, which is more important at nighttime. N<sub>2</sub>O<sub>5</sub> forms from the reactions of NO<sub>2</sub>,  
56 O<sub>3</sub> and NO<sub>3</sub> and hydrolyzes to produce particulate nitrate. They can be summarized as  
57 reactions R1-R5 (Ying et al., 2011; Wang et al., 2018; Li et al., 2018):





63 However, current chemistry transport models (CTM, such as CMAQ, WRF-Chem etc.)  
64 still can't accurately capture the spatiotemporal distributions of nitrate despite of  
65 involving above chemical mechanism. For example, Chang et al. (2018) showed that  
66 the simulated nitrate concentrations derived from default CMAQ (version 5.0.2) were  
67 1.79 to 1.95 times of the observations in summer at two sites adjacent to Beijing. Chen  
68 et al. (2017) found the high uncertainty (about 20%~50%) of simulated nitrate  
69 concentration using CMAQ in Dezhou city (Shandong province, adjacent to Beijing),  
70 which attributed to the unclear mechanism of nitrate formation. Fu et al. (2017) also  
71 found that default CMAQ (version 5.0.1) overestimated the simulated nitrate  
72 concentrations in Beijing-Tianjin-Hebei region.

73 Some studies attributed the overestimation of nitrate to the missing of chlorine  
74 chemical mechanism. According to the field measurements in June 2017 in Beijing  
75 (Zhou et al., 2018), the concentrations of reactive  $\text{Cl}_2$  and  $\text{ClNO}_2$  reached up to 1000  
76 pptv and 1200 pptv, respectively, during some severe air pollution period in summer.  
77 The corresponding concentrations of  $\text{N}_2\text{O}_5$  and nitrate rise up to 700pptv and  $5\mu\text{g m}^{-3}$   
78 from about 40 pptv and  $1\mu\text{g m}^{-3}$ , which were significantly higher than those in coastal  
79 cities and the lower atmosphere in the remote Arctic region (Spicer et al., 1998; Li et  
80 al., 2017; Glasow et al., 2010; Liu et al., 2017). Some studies suggested that the reaction  
81 R5 should be revised as R6 due to the heterogeneous reaction of  $\text{N}_2\text{O}_5$  on chlorine-  
82 containing particle surface (CPS)(Wang et al., 2017; Simon et al., 2010; Glasow et al.,  
83 2010):



85 where  $\phi$  represents the yield of  $\text{ClNO}_2$ . By incorporating this reaction into WRF-Chem,  
86 Li et al. (2017) found that the improved model performed better to match the observed  
87 nitrate concentrations in Hongkong during 15 November and 5 December 2013. The  
88 generated gaseous nitryl chloride ( $\text{ClNO}_2$ ) could affect the formation of nitrate



89 indirectly by increasing the atmospheric OH after a series of chemical reactions, which  
90 are briefly summarized into three steps: (1) the photolysis of ClNO<sub>2</sub> produces atom  
91 chlorine (Cl<sup>•</sup>); (2) the reaction of Cl<sup>•</sup> with VOCs produces peroxy radical (HO<sub>2</sub> and  
92 RO<sub>2</sub>); (3) the increased HO<sub>2</sub> and RO<sub>2</sub> prompt the formation of OH by participating into  
93 free radical cycle and NO<sub>x</sub> cycle (Young et al., 2014; Jobson et al., 1994).

94 The reaction of N<sub>2</sub>O<sub>5</sub> is not the only heterogeneous reaction that influences the  
95 nitrate formation. Some other heterogeneous reactions on CPS can also directly or  
96 indirectly affect nitrate formation. For example, the heterogeneous uptake of NO<sub>2</sub> and  
97 NO<sub>3</sub> on CPS can produce nitrate (Abbatt et al., 1998, Rudich et al., 1996). The reactions  
98 of gaseous O<sub>3</sub>, OH, HO<sub>2</sub>, ClNO<sub>2</sub>, hypochlorous acid (HOCl), chlorine nitrate (ClONO<sub>2</sub>)  
99 with CPS can produce Cl<sub>2</sub> and subsequently photolyze to produce Cl<sup>•</sup> (Knipping et al.,  
100 2000; George et al., 2010; Pratte et al., 2006; Deiber et al., 2004; Faxon et al., 2015),  
101 which can further accelerate the OH formation to affect the reaction R1. However, these  
102 heterogeneous reactions are generally missing in most of the current CTMs.

103 Previously, biomass burning, coal combustion, and waste incineration were  
104 identified as the main sources of gaseous and particulate chlorine compounds in China  
105 from International Global Atmospheric Chemistry Program's Global Emissions  
106 Inventory Activity (GEIA) based on the year 1990 and a localized study by Fu et al.  
107 based on the year 2014 (Keene et al., 1999; Fu et al., 2018). However, recent source  
108 apportionment result of PM<sub>2.5</sub> in Beijing showed that the contribution of coal  
109 combustion had extremely decreased from 22.4% in 2014 to 3% in 2017 with the  
110 replacement of nature gas (obtained from official website of Beijing Municipal Bureau  
111 of Statistics, available at <http://edu.bjstats.gov.cn/>). But another important source—  
112 cooking has received attention as its increasingly contribution to PM<sub>2.5</sub> (accounting for  
113 33% of residential sector; obtained from the official source apportionment analysis of  
114 PM<sub>2.5</sub> in Beijing in 2017; see <http://www.bjepb.gov.cn/bjhr-b/index/index.html>).  
115 Moreover, high content of particulate sodium chloride was measured from the source  
116 characterization studies of PM<sub>2.5</sub> released from the cooking source (Zhang et al., 2016).  
117 Thus, it's important to ascertain the relationship between reactive chlorine species and  
118 nitrate.



119 In this study, the Community Multiscale Air Quality (CMAQ) model with an  
120 improved chlorine heterogeneous chemistry is applied to simulate summer nitrate  
121 concentration in Beijing. We then use the sensitivity analyses to evaluate the  
122 contribution of HNO<sub>3</sub> partitioning and heterogenous production to nitrate formation.  
123 The results of this work can improve our understandings on nitrate formation and  
124 provide useful implications on the nitrate pollution control strategies in Beijing.

125

## 126 **2. Emissions, chemical reactions and model description**

### 127 2.1 Emissions

128 Generally, the conventional emission inventories of air pollutants in China only include  
129 the common chemical species, such as SO<sub>2</sub>, NO<sub>x</sub>, VOCs, PM<sub>2.5</sub>, PM<sub>10</sub>, BC, and OC.  
130 No data on chloride compound emissions were included. Recently, the inorganic  
131 hydrogen chloride (HCl) and fine particulate chloride (PCL) emission inventories for  
132 the sectors of coal combustion, biomass burning, and waste incineration were  
133 developed in 2014 (Qiu et al., 2017, Fu et al., 2018, Liu et al., 2018). However the  
134 gaseous chlorine emission was not estimated in these studies. In addition, these studies  
135 did not account for the rapid decrease of coal consumption in recent years in Beijing  
136 (about 75% from 2014 to 2017). More importantly, the cooking source, as one of the  
137 major contributors to particulate chlorine in Beijing, is not included in current chlorine  
138 emission inventories. Thus, we develop a new emission inventory of reactive chlorine  
139 species, which includes HCl, Cl<sub>2</sub> and PCL for the year of 2017.

140 The emission factor method is applied to calculate the emissions of these reactive  
141 chlorine species, which can be expressed as following equations.

$$142 \quad \text{HCl and Cl}_2: \quad E_{i,j} = \sum_{i,j} A_i \times EF_{i,j} \quad (1)$$

$$143 \quad \text{PCL:} \quad E_{i,j} = \sum_{i,j} A_i \times EF_{i,j} \times \eta \quad (2)$$

144 where  $E_{i,j}$  represents the emission of pollutant  $j$  in  $i$  sector.  $A$  represents the activity data,  
145  $EF$  represents the emission factor.  $\eta$  represents the content of PCL in PM<sub>2.5</sub>.

146 In this study, the Cl<sub>2</sub> production is calculated based on the content of Cl in coal,



147 which had been measured by Deng et al (2017). In addition, the methods of emission  
148 calculation on biomass burning, municipal solid waste (MSW) had been detailed  
149 described by Fu et al. (2018), so we focus on demonstrating the calculation process of  
150 cooking source.

151 The cooking emissions are separately estimated due to the differences of  
152 calculation method between social cooking (including school, corporation and  
153 restaurant etc.) and household cooking emissions, which are expressed as equation 3.

$$154 \quad E_j = (V_f \times H_f \times EF_f + V_c \times H_c \times N_c \times n \times EF_c \times (1 - \eta)) \times 365 \quad (3)$$

155 where  $V_f$  is the volume of exhaust gas from household stove, which equals to 2000 m<sup>3</sup>/h,  
156  $H_f$  is the cooking time for a family, which is set as 3h per day.  $EF_f$  is emission factor.  $H_c$   
157 is the cooking time for restaurant, which is set as 6h per day. The  $N_c$  is the number of  
158 restaurant, school and government department.  $V_c$  is the volume of exhaust gas, which  
159 is set as to 8000 m<sup>3</sup>/h.  $n$  is the number of stove for each unit, which equals to 6 for  
160 restaurant and is calculated as the number of students divide 150 for school.  $\eta$  is the  
161 remove efficient of fume scrubbers, a constant of 30% is chose.

162 Activity data, such as coal consumptions, population, crop yields, and production  
163 of each industrial sector are obtained from Beijing Municipal Bureau of Statistics  
164 (available at <http://tjj.beijing.gov.cn/>). This official data shows that coal combustion has  
165 dramatically decrease from more than 2000 Mt from 2014 to 490 Mt in 2017, which  
166 indicates that significant reduction of emissions of air pollutants. Part of localized data  
167 of PCl, such as the content of PCl in PM<sub>2.5</sub> discharged from cooking, power plant and  
168 biomass burning (10%, 1% and 9.0%, respectively), are obtained based on the localized  
169 measurement. Others emission factors are obtained from the study by Fu et al. Finally,  
170 the sectoral emissions of HCl, Cl<sub>2</sub> and PCl, including power plant, industry, residential,  
171 biomass burning, MSW and cooking, are estimated and listed in Table 1. Finally,  
172 estimated HCl, Cl<sub>2</sub> and PCl missions in Beijing are 1.89 Gg, 0.065Gg and 0.63Gg  
173 respectively. Emissions of other species for this study period were derived by Ding et  
174 al. (under-review; emissions are summerized in Table S1).

175 2.2 Chlorine-related heterogeneous reactions



176 In addition to reactions R1 and R5, gas phase reactions of NO<sub>3</sub> with HO<sub>2</sub> or VOCs (R8  
 177 and R9, see Table 2), N<sub>2</sub>O<sub>5</sub> with H<sub>2</sub>O and the heterogeneous reaction of NO<sub>2</sub> with water-  
 178 containing particle are included in current CMAQ model (Zheng et al., 2015). However,  
 179 these heterogeneous reactions in original CMAQ (version 5.0.1) are not related to  
 180 chlorine species. This study revises the reactions R5 and R10 as R6 and R11 by  
 181 considering the impact of heterogeneous uptake on CPS. In reaction R6, the yield of  
 182 ClNO<sub>2</sub> is represented as (Li et al., 2016):

$$\phi_{ClNO_2} = \left( 1 + \frac{[H_2O]}{483 \times [Cl^-]} \right)^{-1} \quad (4)$$

183 where  $\phi_{ClNO_2}$  is the yield of ClNO<sub>2</sub>, [H<sub>2</sub>O] and [Cl<sup>-</sup>] are the molarities of liquid water  
 184 and chloride in aerosol volume (mol/m<sup>3</sup>).

185 In addition, Laboratorial observations confirmed that heterogeneous uptakes of  
 186 some oxidants (such as O<sub>3</sub> and OH) and reactive chlorine species (such as ClNO<sub>2</sub>, HOCl,  
 187 and ClONO<sub>2</sub>) could occur on CPS to produce Cl<sub>2</sub> (R13-R18), which affected the  
 188 atmospheric OH level after a series of chemical reactions. Note that the products from  
 189 heterogeneous uptake of ClNO<sub>2</sub> on CPS vary with particle acidity. It generates Cl<sub>2</sub> under  
 190 the condition of pH lower than 2 while produces nitrate when the pH is higher than 2.  
 191 These heterogeneous reaction rates are parameterized as first-order reactions, with the  
 192 rate of change of gas phase species concentrations determined by equations (2) (Ying  
 193 et al., 2015):

$$\frac{dC}{dt} = -\frac{1}{4}(\bar{c}\gamma A)C = -k^1 C \quad (5)$$

194 where  $C$  represents the concentration of species,  $\bar{c}$  represents its thermal velocity (m  
 195 s<sup>-1</sup>),  $A$  represents aerosol surface area concentration (m<sup>2</sup> m<sup>-3</sup>),  $\gamma$  represents the uptake  
 196 coefficient. Thus,  $k^1$  is considered as a constant. The parameters of  $A$  and  $\bar{c}$  are  
 197 calculated by CMAQ. Considering the consumption and generation of ClNO<sub>2</sub>, the  
 198 concentration of ClNO<sub>2</sub> can be calculated with equation (3):

$$\begin{aligned} \frac{d[ClNO_2]}{dt} &= -k_1^1[ClNO_2] + k_6^1\phi_{ClNO_2}[N_2O_5] \\ &= -k_1^1[ClNO_2] + k_6^1\phi_{ClNO_2}[N_2O_5]_0 \exp(-k_6^1 t) \end{aligned} \quad (6)$$

199 Assuming  $\phi_{ClNO_2}$  is a constant, an analytical solution can be found for equation (7).



$$[\text{ClNO}_2] = [\text{ClNO}_2]_0 \exp(-k_1^I t) + \frac{k_6^I \phi_{\text{ClNO}_2} [\text{N}_2\text{O}_5]_0}{k_1^I - k_6^I} [\exp(-k_6^I t) - \exp(-k_1^I t)] \quad (7)$$

200 Where  $k_1^I$  represents the reaction constant of reaction R17 or R18. The variable  $t$   
 201 represents the time.

202 The uptake coefficients  $\gamma$  of gaseous species are obtained from published  
 203 laboratorial studies. In the original CMAQ, the uptake coefficient of  $\text{N}_2\text{O}_5$  is determined  
 204 as a function of the concentrations of  $(\text{NH}_4)_2\text{SO}_4$ ,  $\text{NH}_4\text{HSO}_4$  and  $\text{NH}_4\text{NO}_3$  (Davis et al.,  
 205 2008). In this study, the  $\text{Cl}^-$  and  $\text{NO}_3^-$  concentration dependent parameterization (eq. 8)  
 206 by Bertram et al. for  $\text{N}_2\text{O}_5$  is used instead (Bertram et al., 2009). For frozen particles,  
 207 the uptake coefficient is limited to 0.02, as used in the original CMAQ model.

$$\gamma_{\text{N}_2\text{O}_5} = \begin{cases} 0.02, & \text{for frozen aerosols} \\ \frac{4V}{vS} K_h K_f \left( 1 - \frac{1}{\left(\frac{K_3[\text{H}_2\text{O}]}{K_2[\text{NO}_3^-]} + 1 + \left(\frac{K_4[\text{Cl}^-]}{K_2[\text{NO}_3^-]}\right)}\right)} \right) & \end{cases} \quad (8)$$

208 In the above equation,  $V$  represents the particle volume concentration ( $\text{m}^3 \text{m}^{-3}$ );  $S$   
 209 represents the particle surface area concentration ( $\text{m}^2 \text{m}^{-3}$ );  $v$  represents the thermal  
 210 velocity of  $\text{N}_2\text{O}_5$  ( $\text{m s}^{-1}$ );  $K_h$  represents the dimensionless Henry's law coefficient.  $K_f$   
 211 represents a parameterized function based on water concentration and  $K_3/K_2$  and  $K_4/K_2$   
 212 are constants obtained by fitting data. The uptake coefficient of OH is expressed with a  
 213 function of the concentration of  $\text{Cl}^-$  following the IUPAC (International Union of Pure  
 214 and Applied Chemistry) (available at [http://iupac.poleether.fr/htdocs/datasheets/pdf/O-](http://iupac.poleether.fr/htdocs/datasheets/pdf/O-H_halide_solutions_VIA2.1.pdf)  
 215 [H\\_halide\\_solutions\\_VIA2.1.pdf](http://iupac.poleether.fr/htdocs/datasheets/pdf/O-H_halide_solutions_VIA2.1.pdf)).

$$\gamma = \min\left(0.04 \times \frac{[\text{Cl}^-]}{1000 \times M}, 1\right) \quad (9)$$

216 where  $M$  represents the volume of liquid water in aerosol volume ( $\text{m}^3/\text{m}^3$ ).

217 The uptake coefficients of  $\text{O}_3$ ,  $\text{NO}_3$ ,  $\text{NO}_2$ ,  $\text{HOCl}$ ,  $\text{ClNO}_2$ , and  $\text{ClONO}_2$  are treated  
 218 as constants. Among of them, the  $\gamma$  value of  $\text{NO}_3$ ,  $\text{NO}_2$ ,  $\text{HOCl}$  and  $\text{ClONO}_2$  are set as  
 219  $3 \times 10^{-3}$ ,  $1 \times 10^{-4}$ ,  $1.09 \times 10^{-3}$  and 0.16 based on the laboratory measurements (Rudich et  
 220 al., 1996; Abbatt et al., 1998; Pratte et al., 2006; Gebel et al., 2001). A preliminary value  
 221 of  $10^{-3}$  in the daytime and  $10^{-5}$  at nighttime is chosen for the  $\text{O}_3$  uptake coefficient  
 222 (Keene et al., 1999). The uptake coefficient of  $\text{ClNO}_2$  depends on the particle acidity,  
 223 with the value of  $2.65 \times 10^{-6}$  for reaction R17 and  $6 \times 10^{-3}$  for reaction R18 (Robert et



224 al., 2008).

225 2.4 CMAQ model configuration

226 These heterogeneous reactions of chlorine are incorporated into revised CMAQ  
227 (version 5.0.1) to simulate the distribution of nitrate concentration in Beijing in June.

228 The gas phase chemical mechanism is based on the SAPRC-11 with a comprehensive  
229 gas-phase chemistry of chlorine (Cater et al., 2012; Ying et al., 2015). Three-level  
230 nested domains with the resolutions of 36km, 12km, and 4km using Lambert Conformal  
231 Conic projection (173×136, 135×228 and 60×66 grid cells) are chosen in this work (see  
232 Figure 3 for the inner most domain). The two true latitudes is set as 25 °N and 40°E and  
233 the origin of the domain is set as 34°N, 110°E. The left-bottom coordinates of the  
234 outmost domain are positioned at x = -3114 km, y = -2448 km. The BASE case  
235 (simulation using default CMAQ) and HET case (with improved CMAQ) are compared  
236 to evaluate the impact of heterogeneous chlorine chemistry on nitrate formation.

237

### 238 **3. Results**

#### 239 3.1 Model performance evaluation

240 Predicted hourly Cl<sub>2</sub>, ClNO<sub>2</sub> and N<sub>2</sub>O<sub>5</sub> concentrations were compared with  
241 observations measured at the Institute of Atmospheric Physics (IAP), Chinese Academy  
242 of Sciences (39.98N°, 116.37E°) using a high-resolution time-of-flight chemical  
243 ionization mass spectrometer (CIMS) from 11 to 15 June 2017 (for site description,  
244 instrument introduction, and analytical method, please refer to the study by Zhou et al.  
245 (2018)). Figure 1 shows that the concentrations of Cl<sub>2</sub> and ClNO<sub>2</sub> in BASE case are  
246 rather low (close to 0), proving that the gas-phase chemistry is not the major pathway  
247 to produce Cl<sub>2</sub> and ClNO<sub>2</sub>. By contrast, the simulated Cl<sub>2</sub> and ClNO<sub>2</sub> concentrations in  
248 HET case increase significantly, correspondingly the NMB and NME changes from -  
249 100% to -54% and 100% to 61% for Cl<sub>2</sub>, and from -100% to -58% and 100% to 62%  
250 for ClNO<sub>2</sub>, respectively (the parameter of total particle surface area (TOTSURFA) in  
251 CMAQ is revised by multiplying a factor of 5 in daytime and 10 in nighttime because  
252 this parameter is underestimated compared with the study of Zhou et al. (2018)). The



253 simulations of  $\text{Cl}_2$  and  $\text{ClNO}_2$  are improved because the newly added heterogeneous  
254 reactions prompt the conversions of chlorine from particle state to gaseous state.  
255 Overall, the  $\text{Cl}_2$  and  $\text{ClNO}_2$  concentrations are still underestimated. The  
256 underestimation of  $\text{Cl}_2$  may be associated with insufficient chemical conversion from  
257  $\text{ClNO}_2$  to produce  $\text{Cl}_2$  at nighttime. The uncertainty in the uptake coefficient of  $\text{O}_3$  in  
258 daytime could also be an important factor as we believe that the uptake of  $\text{O}_3$  is the  
259 major source of  $\text{Cl}_2$  during this period of time (see discussion in Section 3.2). According  
260 to equation (7), the underestimation of  $\text{ClNO}_2$  concentration may be due to two factors,  
261 that is, reaction rate  $K_6$  and  $\text{N}_2\text{O}_5$  concentration. Because the  $\text{N}_2\text{O}_5$  concentration is not  
262 substantially underestimated (see Figure 1(c)), we believe that the deviation of reaction  
263 rate  $K_6$  is the culprit to result in the underestimation of  $\text{ClNO}_2$ , thus the uptake  
264 coefficient of  $\text{N}_2\text{O}_5$  which significantly affects  $K_6$  may be an important factor to affect  
265 the accuracy of  $\text{ClNO}_2$  simulation (see further discussion in Section 3.2). The improved  
266 CMAQ can accurately capture the diurnal variation of  $\text{N}_2\text{O}_5$  concentration as well as  
267 the peak values (Figure 1(c)). In general, although the overall NMB and NME of BASE  
268 case (-20% and 38%) are slightly better than the HET case (-21% and 41%), the  
269 improved CMAQ (with the NMB and NME of -3% and 14%) perform better than  
270 original CMAQ (with the NMB and NME of -33% and 52%) in some period of heavy  
271 air pollution (such as the nighttime on 12 June and 13 June).

272 Predicted  $\text{NO}_3^-$  and  $\text{PCL}$  concentrations are compared with observations measured  
273 at an adjacent monitoring site located at the rooftop of School of Environment building  
274 in Tsinghua University (THU, 40.00N°, 116.34E°, about 5 km from IAP) using an  
275 Online Analyser of Monitoring of Aerosol and Gases (MARGA) from 11 to 15 June  
276 2017. According to Figure 1(d), excluding the very high nitrate level in 13 June, the  
277 simulated nitrate concentration is commonly lower than the observations, probably as  
278 the result of the unreasonable  $\text{NH}_3$  gas-particle partitioning model in our developed  
279 CMAQ model (Song et al., 2018). Comparing with the very high nitrate concentrations  
280 in 12 June and 13 June, we find that the simulated nitrate concentration using improved  
281 CMAQ is superior to use original CMAQ, while the nitrate level is higher in daytime  
282 and lower in nighttime, with the NMB and NME improve from -10% and 46% to -5%



283 and 39%. Excluding the daytime on 15 June, the improved CMAQ also capture the  
284 hourly variation of PCl concentration and perform better than using original CMAQ,  
285 correspondingly the NMB and NME change from -48% and 72% to -37% and 67%.  
286 The substantial underestimation of PCl in the daytime on 15 June is likely caused by  
287 some local emissions during this period.

288

### 289 3.2 Estimation of uptake coefficients of O<sub>3</sub> and N<sub>2</sub>O<sub>5</sub>

290 The uptake coefficients of O<sub>3</sub> and N<sub>2</sub>O<sub>5</sub> may be important factors affecting the accuracy  
291 of simulated nitrate concentrations. Some studies have confirmed that the reaction of  
292 O<sub>3</sub> on CPS can indirectly affect the nitrate formation by increasing the atmospheric Cl<sub>2</sub>  
293 and OH level (Li et al., 2016; Liu et al., 2018). According to Figure 1(a), the improved  
294 model still substantially underestimates the concentration of Cl<sub>2</sub>, which may be  
295 associated with the underestimation of the uptake coefficient of O<sub>3</sub>. The uptake  
296 coefficient of O<sub>3</sub> used in this study is empirical and has not been confirmed by  
297 laboratory studies. The uptake coefficients were increased by a factor of 10 (0.01 for  
298 daytime and 10<sup>-4</sup> for nighttime) to evaluate the sensitivity of Cl<sub>2</sub> production and nitrate  
299 formation. Figure 2 shows that the simulated Cl<sub>2</sub> and nitrate concentrations in daytime  
300 increase significantly (especially for Cl<sub>2</sub>) and sometimes can capture the peak value  
301 (such as the daytime peak on 14 June). However, although the NMB and NME of Cl<sub>2</sub>  
302 and nitrate improve from -18% and 39% to 1% and 28% when the new uptake  
303 coefficients are used, the simulated Cl<sub>2</sub> concentrations are still quite different from the  
304 observations such as during the daytime in 11 and 12 June, see Figure 2). A non-  
305 constant parameterization of the uptake coefficients of O<sub>3</sub> that consider the influence of  
306 PCl concentrations, meteorology conditions, etc., similar to those of OH and N<sub>2</sub>O<sub>5</sub>,  
307 might be needed. Further laboratory studies should be conducted to confirm this  
308 conclusion.

309 As described above, the uptake coefficient of N<sub>2</sub>O<sub>5</sub> can be expressed in multiple  
310 forms. In addition to the parameterization of Bertram et al. (2009) used in the HET case,  
311 two additional simulations were performed to assess the impact of uptake coefficient of  
312 N<sub>2</sub>O<sub>5</sub> on nitrate formation: (1) using the original CMAQ parameterization of Davis et



313 al.(2008), and (2) the maximum value of 0.09 from the study by Zhou et al. (2018). The  
314 results show that the HET case has better agreement with the observations than the two  
315 additional simulations (Table 3). The Davis et al. parameterization is dependent on the  
316 concentration of nitrate and sulfate concentration, which is inferior to the coefficient  
317 used in this study. We conclude that a chlorine-related coefficient is more reasonable for  
318 the application of simulating reactive chlorine species and nitrate concentrations in high  
319 chlorine emission region. Using the uptake coefficient of 0.09 can generally increase  
320 the concentration of nitrate in some periods, but it also leads to significant  
321 overestimations of the nitrate level (such as nighttime on 12-13 June and 13-14 June).

322

### 323 3.3 Spatial distributions of nitrate and chlorine species concentrations

324 The distributions of averaged  $\text{Cl}_2$ ,  $\text{ClNO}_2$ ,  $\text{N}_2\text{O}_5$  and  $\text{NO}_3^-$  concentration from 11 to 15  
325 June in the BASE case and HET case are shown in Figure 3. Compared to original  
326 CMAQ, the averaged concentrations of  $\text{Cl}_2$  and  $\text{ClNO}_2$  derived from improved CMAQ  
327 increase significantly in the eastern region of Beijing, reaching up to 23 ppt and 71 ppt  
328 from near zero. High concentrations are not found in southern region with intensive  
329 emissions of chlorine species, implying that  $\text{Cl}_2$  and  $\text{ClNO}_2$  are easy to transport among  
330 cities .

331 The spatial distribution of  $\text{N}_2\text{O}_5$  concentration in nighttime differs from that of  
332 other species. While the concentrations of most of the species are higher in the southern  
333 region, the  $\text{N}_2\text{O}_5$  concentration is low in some parts of this region. This is because the  
334  $\text{O}_3$  concentration in the core urban areas is low due to high  $\text{NO}_x$  emissions. By  
335 incorporating the chlorine heterogeneous reaction, the  $\text{N}_2\text{O}_5$  concentrations decrease by  
336 about 16% because more  $\text{N}_2\text{O}_5$  is converted into nitrate. Although the added PCl  
337 prompts the conversion from  $\text{N}_2\text{O}_5$  to nitrate, the nitrate concentration in these regions  
338 has not presented significant increase. In contrast, the nitrate concentration decreases  
339 significantly by about 22% due to the reduction of 2 mol  $\text{NO}_3^-$  in R5 to 1 mol in R6 for  
340 each mole of  $\text{N}_2\text{O}_5$  reacted. Although the generated  $\text{ClNO}_2$  also further produces nitrate,  
341 the particle pH in most time is higher than 2 (see Figure S1) and the uptake coefficient  
342 of  $\text{ClNO}_2$  is significantly lower than  $\text{N}_2\text{O}_5$  (0.01~0.09 for  $\text{N}_2\text{O}_5$  and  $6 \times 10^{-3}$  for  $\text{ClNO}_2$ ),



343 leading to an overall decrease of nitrate production.

344

345 3.4 Relationship between nitrate formation and chlorine chemistry

346 A CMAQ-tagged method (tagging the nitrate concentration produced by the  
347 heterogeneous reaction, the rest of nitrate is produced by HNO<sub>3</sub> partitioning) is used to  
348 estimate the nitrate production from heterogeneous pathways and HNO<sub>3</sub> partitioning  
349 pathways. In general, about 58.3% of nitrate originates from HNO<sub>3</sub> partitioning and  
350 41.7% of nitrate are produced from heterogeneous reaction (Figure 4). This conclusion  
351 generally agrees with measurements at a nearby observation site in Peking University  
352 (PKU) (Wang et al., 2017), which indicates 52% from the heterogeneous process and  
353 48% from HNO<sub>3</sub> partitioning. Two factors may lead to the differences between our  
354 simulation and the measurement at PKU. One is the chlorine heterogeneous chemistry  
355 and the other is the pollution level. More nitrate is expected to be produced by HNO<sub>3</sub>  
356 gas-to-particle partitioning in cleaner days whereas the heterogeneous process is more  
357 important in haze days. The averaged nitrate level at PKU site during the measurement  
358 was 14.2 μg m<sup>-3</sup>, about 4 times higher than that in this study.

359 The production rates of gaseous HNO<sub>3</sub> from different gas-phase reactions and  
360 nitrate formation from different heterogeneous reaction pathways in the BASE case and  
361 HET case are further studied using process analysis. Figure 4 shows that the reaction  
362 of OH and NO<sub>2</sub> is always the major pathway to produce gaseous HNO<sub>3</sub> regardless of  
363 daytime or nighttime. However, its reaction rate decreases significantly from daytime to  
364 nighttime (from 1272 ppt h<sup>-1</sup> to 234 ppt h<sup>-1</sup> on average). The other HNO<sub>3</sub> production  
365 pathways in daytime can be ignored because their reaction rates are rather low. But at  
366 nighttime the reaction rate of N<sub>2</sub>O<sub>5</sub> with water vapor presents a rapid increase, reaching  
367 up to 12.2 ppt h<sup>-1</sup> from 1.7 ppt h<sup>-1</sup>, which accounts for approximately 5% of the HNO<sub>3</sub>  
368 formation in the gas phase. For the heterogeneous pathways, all of the reactions can be  
369 neglected in the daytime. At nighttime, the heterogeneous uptake N<sub>2</sub>O<sub>5</sub> on the particle  
370 surface is the major pathway to nitrate formation (about 3.07 μg m<sup>-3</sup> h<sup>-1</sup>, account for  
371 84.8% in heterogeneous formation). By contrast, heterogeneous uptake of NO<sub>2</sub> on  
372 particulate H<sub>2</sub>O has less contribution to nitrate (15.2%).



373           When the chlorine chemistry is included, the gaseous  $\text{HNO}_3$  produced by OH  
374 reacting with  $\text{NO}_2$  increases significantly (up to  $1487 \text{ ppb h}^{-1}$  in the daytime and  $253$   
375  $\text{ppt h}^{-1}$  at nighttime) due to increased atmospheric OH concentrations predicted by the  
376 chlorine reactions. Similar conclusions are also obtained by Li et al. (2016) and Liu et  
377 al. (2017) based on observations and model simulation. Note that the reaction of  $\text{NO}_3$   
378 with  $\text{HO}_2$  does not increase obviously even through the chlorine chemistry also leads  
379 to higher atmospheric  $\text{HO}_2$  levels (increase by more than 20%, Li et al., (2016)) because  
380 the atmospheric  $\text{NO}_3$  radical level is rather low. The heterogeneous production of nitrate  
381 from the reaction of  $\text{N}_2\text{O}_5$  uptake decreases dramatically (about 27%) due to the  
382 inclusion of heterogeneous reactions of chlorine species. The contributions of  $\text{NO}_2$   
383 uptake to nitrate also decrease by 22% because of the lower rate constant of the reaction  
384 of  $\text{NO}_2$  with PCl. In contrast, the contribution of  $\text{ClNO}_2$  decomposition to nitrate  
385 production increases by 6% in the HET case. Generally, the overall nitrate  
386 concentrations estimated by original CMAQ is about 22% higher than the modified  
387 CMAQ during this study period.

388

#### 389 **4. Conclusions**

390 Current chemistry transport models are evaluated to have high uncertainty in the  
391 simulation of nitrate, especially for the period of heavy air pollution. In this work, an  
392 improved CMAQ model incorporated with chlorine heterogeneous chemistry is  
393 developed to evaluate the impact of chlorine-related heterogeneous reaction on nitrate  
394 formation and quantify the contributions from gas-to-particle partitioning of  $\text{HNO}_3$  and  
395 from different heterogeneous reactions.

396           This results show four meaningful conclusions: (1) the emission inventories of  
397 reactive chlorine species are important because it is the cornerstones of studying chlorine  
398 chemistry; (2) The sensitivity analysis shows that a non-constant parameterization of  
399 the uptake coefficients of  $\text{O}_3$  that consider the influence of PCl concentrations,  
400 meteorology conditions, etc., might be needed,  $\text{N}_2\text{O}_5$  uptake coefficient expressed as a  
401 function of the concentrations of chlorine can capture the nitrate concentration better  
402 than others; (3)  $\text{Cl}_2$  and  $\text{ClNO}_2$  are easy to transport among cities because high



403 concentrations of them are not found in southern region with intensive emissions of  
404 chlorine species. (4) more importantly, current CTMs without a complete treatment of  
405 the chlorine chemistry can significantly underestimate the nitrate level from  $\text{HNO}_3$   
406 partitioning due to underestimation of the reaction rate of OH with  $\text{NO}_2$  and  
407 overestimate the heterogeneous formation due to missing chlorine heterogeneous  
408 chemistry.

409 This study aims to improve our understandings on the chlorine chemistry and its  
410 impact on nitrate formation, which can provide useful implications on the nitrate  
411 pollution control strategies for those regions that suffered serious nitrate pollution.

412

413 **Data availability.** The data in this study are available from the authors upon request  
414 ([shxwang@tsinghua.edu.cn](mailto:shxwang@tsinghua.edu.cn))

415

416 **Author contributions.** SW, and JH conducted the study; XQ, QY, SW, LD and JX wrote  
417 the paper. JZ, DD, YS, BL, AS, XY and QX analyzed data.

418

419 **Competing interests.** The authors declare that they have no conflict of interest.

420

421 **Acknowledgements.** This work was supported by National Natural Science Foundation  
422 of China (21625701), China Postdoctoral Science Foundation (2018M641385),  
423 National Research Program for Key Issue in Air Pollution Control (DQGG0301,  
424 DQGG0501) and National Key R&D Program of China (2018YFC0213805,  
425 2018YFC0214006). The simulations were completed on the “Explorer 100” cluster  
426 system of Tsinghua National Laboratory for Information Science and Technology.

427 **References**

- 428 Abbatt, J. P., Waschewsky, G. C., et al.: Heterogeneous interactions of HOBr, HNO<sub>3</sub>, O<sub>3</sub>, and NO<sub>2</sub>  
429 with deliquescent NaCl aerosols at room temperature. *J. Phys. Chem. A.*, 102, 3719-3725, 1998.
- 430 Bertram, T. H., Thornton, J. A.: Toward a general parameterization of N<sub>2</sub>O<sub>5</sub> reactivity on aqueous  
431 particles: the competing effects of particle liquid water, nitrate and chloride. *Atmos. Chem.*  
432 *Phys.*, 9, 8351-8363, 2009.
- 433 Cater, W. P. L., Heo, G.: Development of revised SAPRC aromatics mechanisms. Final Report to  
434 the California Air Resources Board, Contracts No. 07-730 and 08-326, April 12, 2012
- 435 Chang, X., Wang, S., Zhao, B., et al.: Assessment of inter-city transport of particulate matter in the  
436 Beijing-Tianjin-Hebei region, *Atmos. Chem. Phys.*, 18, 4843-4858,  
437 <https://doi.org/10.5194/acp-18-4843-2018>, 2018.
- 438 Chen, D.S., Liu, X.X., Lang, J.L., et al.: Estimating the contribution of regional transport to PM<sub>2.5</sub>  
439 air pollution in a rural area on the North China Plain. *Sci. Total. Environ.*, 583, 280-291, 2017.
- 440 Davis, J. M., Bhave, P. V., Foley, K. M.: Parameterization of N<sub>2</sub>O<sub>5</sub> reaction probabilities on the  
441 surface of particles containing ammonium, sulfate, and nitrate. *Atmos. Chem. Phys.* 8, 5295-  
442 5311, 2008.
- 443 Deng, S., Zhang, C., Liu, Y., et al.: A Full-Scale Field Study on Chlorine Emission of Pulverized  
444 Coal-Fired Power Plants in China. *Research of Environmental Science*. In Chinese, 27, 127-  
445 133, 2014.
- 446 Deiber, G., George, C., Le Calve, S., Schweitzer, F., Mirabel, P.: Uptake study of ClONO<sub>2</sub> and  
447 BrONO<sub>2</sub> by Halide containing droplets. *Atmos. Chem. Phys.* 4, 1291-1299, 2004.
- 448 Faxon, C. B., Bean, J. K., Hildebrandt R.L.: Inland Concentrations of Cl<sub>2</sub> and ClONO<sub>2</sub> in Southeast  
449 Texas Suggest Chlorine Chemistry Significantly Contributes to Atmospheric Reactivity.  
450 *Atmosphere*, 6, 1487-1506, 2015.
- 451 Fu, X., Wang, S.X., Xing, J., et al.: Increasing Ammonia Concentrations Reduce the Effectiveness  
452 of Particle Pollution Control Achieved via SO<sub>2</sub> and NO<sub>x</sub> Emissions Reduction in East China.  
453 *Environ. Sci. Technol. Lett.* 4, 221-227, 2017.
- 454 Fu, X., Wang, T., Wang, S. X., et al.: Anthropogenic Emissions of Hydrogen Chloride and Fine  
455 Particulate Chloride in China. *Environ. Sci. Technol.* 52, 1644-1654, 2018.
- 456 George, I. J., Abbatt, J. P.: Heterogeneous oxidation of atmospheric aerosol particles by gas-phase  
457 radicals. *Nat. Chem.* 2, 713-722, 2010.
- 458 Gebel, M. E., Finlayson-Pitts, B. J.: Uptake and reaction of ClONO<sub>2</sub> on NaCl and synthetic sea salt.  
459 *J. Phys. Chem. A*, 105, 5178-5187, 2001.
- 460 Glasow, V.R. Atmospheric chemistry: wider role for airborne chlorine. *Nature*. 464, 168-169. 2010.
- 461 Li, H.Y., Zhang, Q., Zheng, B., et al.: Nitrate-driven urban haze pollution during summertime over  
462 the North China Plain. *Atmos. Chem. Phys.*, 18, 5293-5306, 2018.
- 463 Li, Q.Y., Zhang, L., Wang, T., et al. Impacts of heterogeneous uptake of dinitrogen pentoxide and  
464 chlorine activation on ozone and reactive nitrogen partitioning: improvement and application  
465 of the WRF-Chem model in southern China. *Atmos. Chem. Phys.*, 16, 14875-14890, 2016.
- 466 Liu, X. X., Qu, H., Huey, L. G., et al.: High Levels of Daytime Molecular Chlorine and Nitryl  
467 Chloride at a Rural Site on the North China Plain. *Environ. Sci. Technol.*, 51, 9588-9595, 2017.
- 468 Liu, Y.M., Fan, Q., Chen, X.Y.: Modeling the impact of chlorine emissions from coal combustion  
469 and prescribed waste incineration on tropospheric ozone formation in China. *Atmos. Chem.*  
470 *Phys.*, 18, 2709-2724, 2018.



- 471 Keene, W. C., Khalil, M. A. K., Erickson, D. J., et al.: Composite global emissions of reactive  
472 chlorine from anthropogenic and natural sources: Reactive Chlorine Emissions Inventory. *J.*  
473 *Geophys. Res.-Atmos.*, 104, 8429-8440, 1999.
- 474 Jobson, B. T., Niki, H., Yokouchi, Y., et al.: Measurements of C2-C6 hydrocarbons during the Polar  
475 Sunrise 1992 experiment: Evidence for Cl atom and Br atom chemistry, *J. Geophys. Res.*, 99,  
476 25355-25368, 1994.
- 477 Keene, W. C.; Pszenny, A. A. P.; Jacob, D. J.; Duce, R. A.; Galloway, J. N.; Schultz-Tokos, J. J.;  
478 Sievering, H.; Boatman, J. F.: The Geochemical Cycling of Reactive Chlorine through the  
479 Marine Troposphere. *Global. Biogeochem.*, 4, 407-430, 1990.
- 480 Knipping, E. M., Lakin, M. J., Foster, K. L., Jungwirth, P., Tobias, D. J., Gerber, R. B., Dabdub, D.,  
481 Finlayson-Pitts, B. J.: Experiments and simulations of ion-enhanced interfacial chemistry on  
482 aqueous NaCl aerosols. *Science*, 288, 301-306, 2000.
- 483 Ma, X.Y., Sha, T., Wang, J.Y., et al.: Investigating impact of emission inventories on PM<sub>2.5</sub>  
484 simulations over North China Plain by WRF-Chem. *Atmos. Environ.*, 195, 125-140. 2018.
- 485 Pratte, P., Rossi, M. J.: The heterogeneous kinetics of HOBr and HOCl on acidified sea salt and  
486 model aerosol at 40-90% relative humidity and ambient temperature. *Phys. Chem. Chem. Phys.*  
487 8, 3988-4001, 2006.
- 488 Qiu, X.H., Chai, F.H., Duan, Lei., et al.: Deriving High-Resolution Emission Inventory of Open  
489 Biomass Burning in China based on Satellite Observations. *Environ. Sci. Technol.*, 50, 11779-  
490 11786, 2017.
- 491 Rudich, Y., Talukdar, R.K., Ravishankara, A.R., et al.: Reactive uptake of NO<sub>3</sub> on pure water and  
492 ionic solutions. *J. Geophys. Res.* 101, 21023-21031, 1996.
- 493 Roberts, J. M., Osthoff, H. D., Brown, S. S., Ravishankara, A. R.: N<sub>2</sub>O<sub>5</sub> oxidizes chloride to Cl<sub>2</sub> in  
494 acidic atmospheric aerosol. *Science*, 321, 1059-1059, 2008.
- 495 Simon, H., Kimura, Y., McGaughey, G., et al.: Modeling heterogeneous ClNO<sub>2</sub> formation, chloride  
496 availability, and chlorine cycling in Southeast Texas. *Atmos. Environ.*, 44, 5476-5488, 2010.
- 497 Spicer, C.W., Chapman, E.G., Finlayson-Pitts, et al.: Unexpectedly high concentrations of  
498 molecular chlorine in coastal air. *Nature*, 394, 353-356, 1998.
- 499 Song, S. J., Gao, M., Xu, W. Q.: Fine-particle pH for Beijing winter haze as inferred from different  
500 thermodynamic equilibrium models. *Atmos. Chem. Phys.*, 18, 7423-7438, 2018.
- 501 Wang, H.C., Lu, K.D., Chen, X.R., et al.: High N<sub>2</sub>O<sub>5</sub> concentrations observed in urban Beijing:  
502 implications of a large nitrate formation pathway. *Environ. Sci. Technol. Lett.* 4, 416-420, 2017.
- 503 Wang, H.C., Lu, K.D., Chen, X.R., et al.: Fast particulate nitrate formation via N<sub>2</sub>O<sub>5</sub> uptake aloft in  
504 winter in Beijing. *Atmos. Chem. Phys.*, 18, 10483-10495, 2018.
- 505 Wen, L., Xue, L.K., Wang, X.F., et al.: Summertime fine particulate nitrate pollution in the North  
506 China Plain: increasing trends, formation mechanisms and implications for control policy.  
507 *Atmos. Chem. Phys.*, 18, 11261-11275, 2018.
- 508 Ying, Q.: Physical and chemical processes of wintertime secondary nitrate aerosol formation.  
509 *Front. Environ. Sci. Eng.*, 5, 348-361, 2011.
- 510 Ying, Q., Li, J. Y., Kota, S. H.: Significant Contributions of Isoprene to Summertime Secondary  
511 Organic Aerosol in Eastern United States. *Environ. Sci. Technol.*, 49, 7834-7842, 2015.
- 512 Young, C.J., Washenfelder, R.A., Edwards, P.M., et al.: Chlorine as a primary radical: evaluation of  
513 methods to understand its role in initiation of oxidative cycles. *Atmos. Chem. Phys.* 14, 3247-  
514 3440, 2014.



- 515 Zhang, T., Peng, L., Li, Y.H.: Chemical characteristics of PM<sub>2.5</sub> emitted from cooking fumes. Res.  
516 Environ. Sci., 29, 183-191, 2016. In Chinese.
- 517 Zheng, B., Zhang, Q., He, K.B., et al.: Heterogeneous chemistry: a mechanism missing in current  
518 models to explain secondary inorganic aerosol formation during the January 2013 haze episode  
519 in North China. Atmos. Chem. Phys., 15, 2013-2049, 2015.
- 520 Zhou, W., Zhao, J., Ouyang, B., et al.: Production of N<sub>2</sub>O<sub>5</sub> and ClNO<sub>2</sub> in summer in urban Beijing,  
521 China., Atmos. Chem. Phys., 18, 11581-11597, 2018.
- 522
- 523



524 **Figure captions**

525

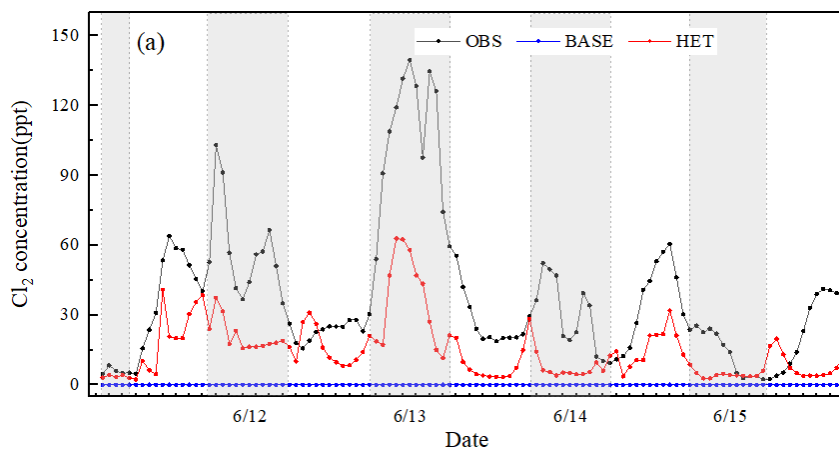
526 Figure 1. Comparison of simulated and observed  $\text{Cl}_2$ ,  $\text{ClNO}_2$ ,  $\text{N}_2\text{O}_5$ ,  $\text{NO}_3^-$  and  $\text{PcI}$  using  
527 original and improved CMAQ (the gray presents nighttime)

528 Figure 2. Comparison of simulated  $\text{Cl}_2$  and  $\text{NO}_3^-$  concentrations under different uptake  
529 coefficient of  $\text{O}_3$  (HET-Co: the scenario of uptake coefficients).

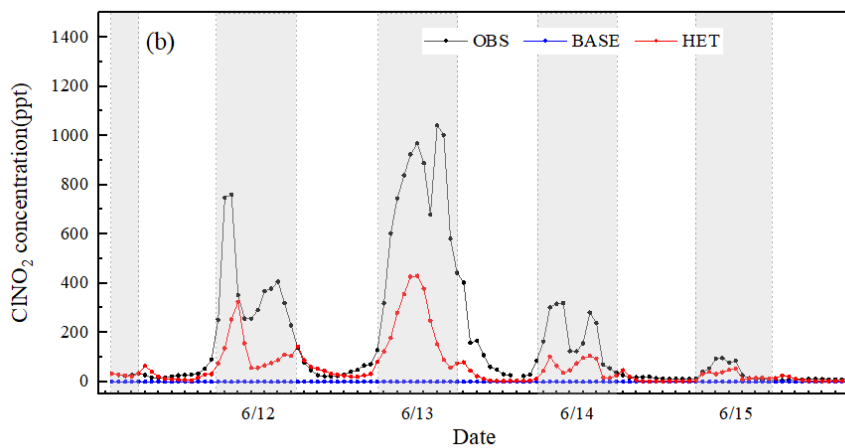
530 Figure 3. Spatial distributions of  $\text{Cl}_2$ ,  $\text{ClNO}_2$ ,  $\text{N}_2\text{O}_5$  and  $\text{NO}_3^-$  concentration in daytime  
531 and nighttime (a-b: concentrations of  $\text{Cl}_2$  and  $\text{ClNO}_2$  in HET case; c-d: the concentration  
532 of  $\text{N}_2\text{O}_5$  in HET case and difference between HET case and BASE case; e-f: the diurnal  
533 concentration of  $\text{NO}_3^-$  in HET case and difference between HET case and BASE case;  
534 g-h: the nocturnal concentration of  $\text{NO}_3^-$  in HET case and difference between HET case  
535 and BASE case).

536 Figure 4. Contributions of different gas-phase reaction pathways and heterogeneous  
537 reaction to nitrate formation.

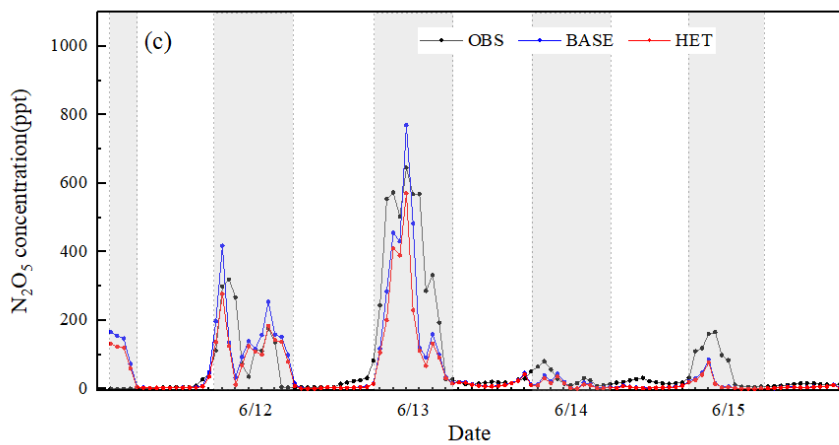
538



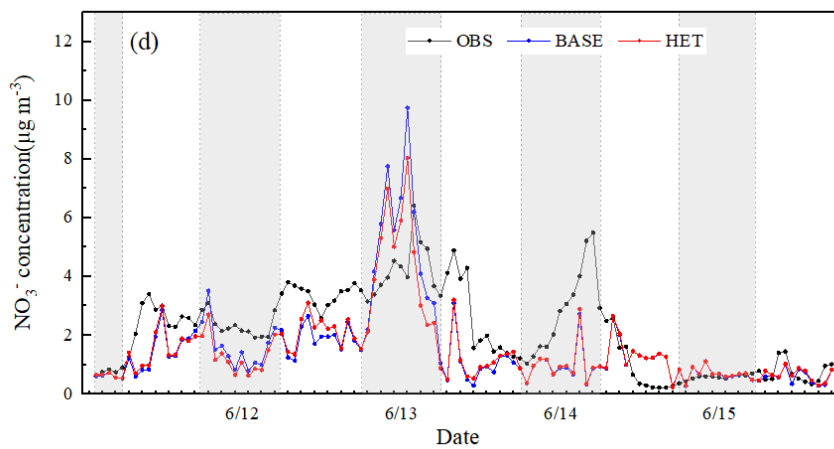
539



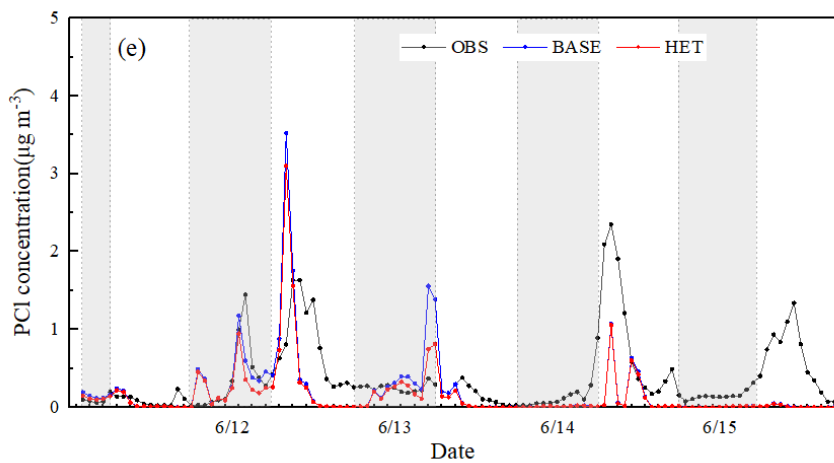
540



541



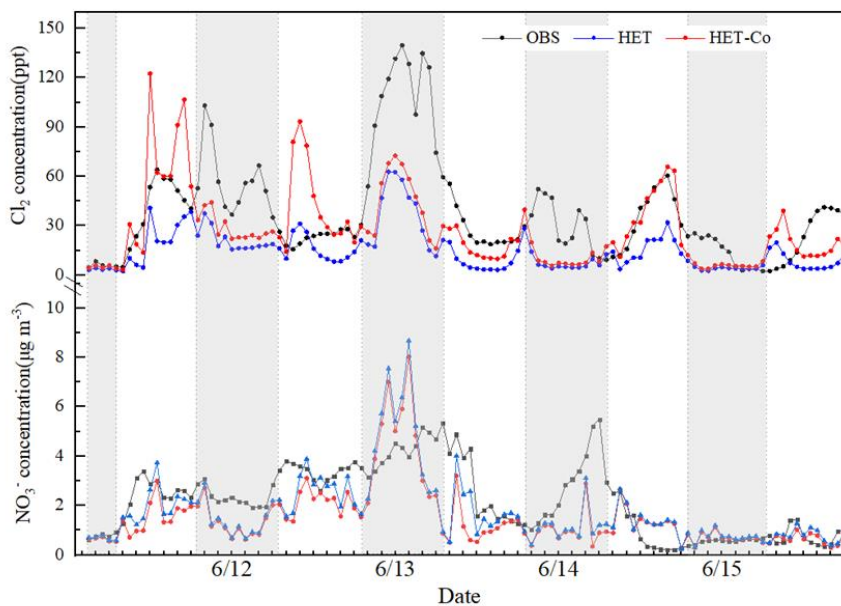
542



543

544 Figure 1

545



546

547 Figure 2

548

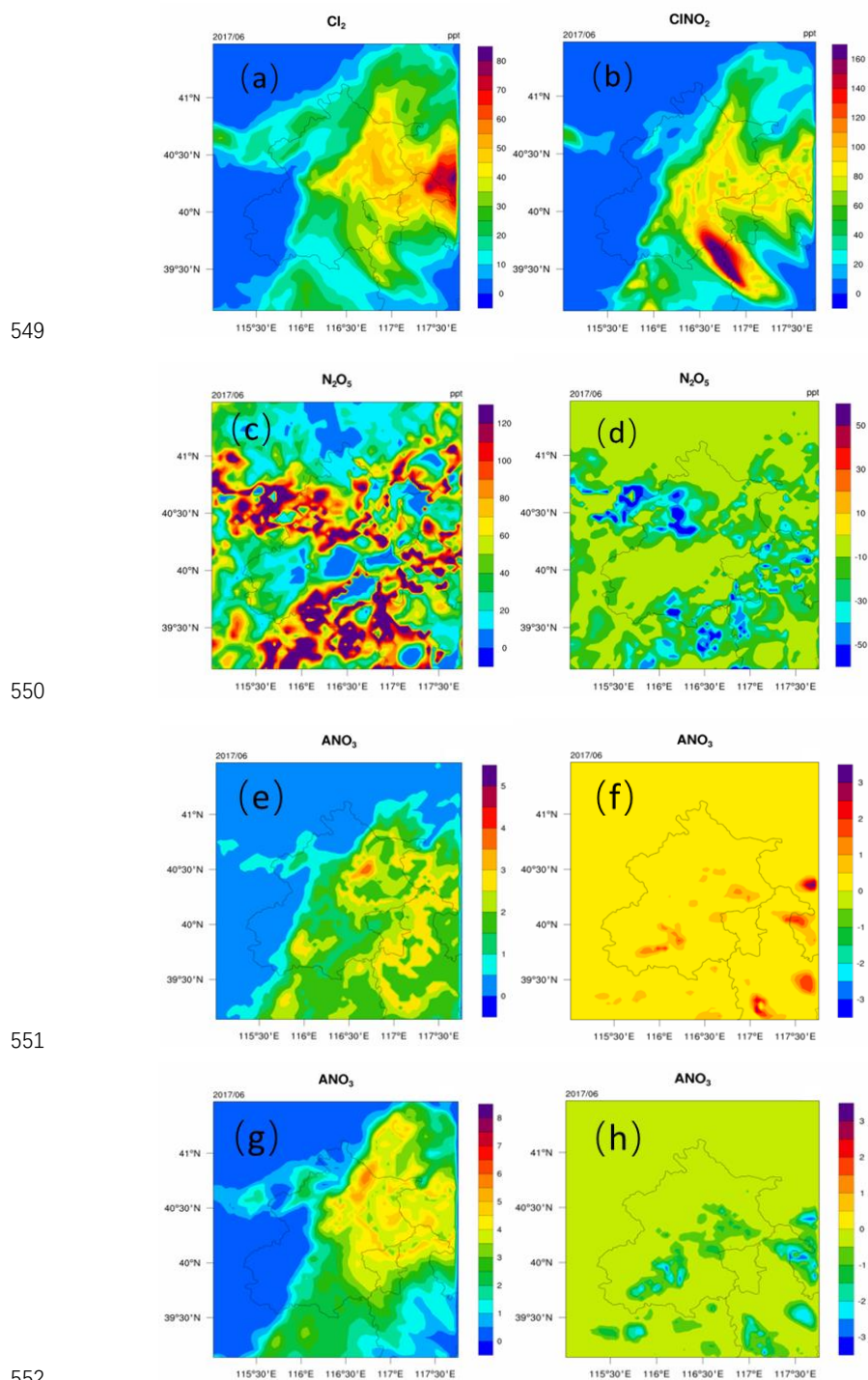
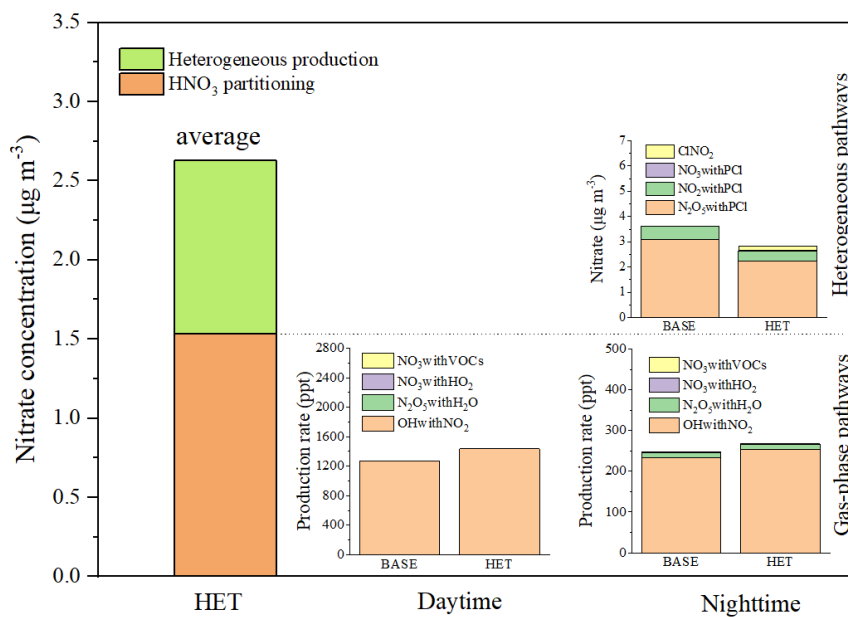


Figure 3



554 Note: the distribution of  $\text{Cl}_2$  and  $\text{ClNO}_2$  in HET minus BASE have not been shown because their  
555 concentrations in BASE case are rather low (close to 0)  
556  
557



558

559 Figure 4

560

561 Table 1 The sectoral emissions of HCl, Cl<sub>2</sub> and PCl. Unit: Mg

Sector	Emissions		
	HCl	Cl <sub>2</sub>	PCl
Power plant	22.8	1.2	6.75
Industry	587.3	20.1	89.2
Residential	202.4	8.1	34.7
Biomass burning	0.182	0	0.14
MSW	1080.2	0	8.47
Cooking	0	0	426.8
Total	1892.9	29.4	566.1

562

563



564 Table 2 Major gas-phase and heterogeneous pathway of producing nitrate in original  
 565 CMAQ and newly added or revised heterogeneous reactions in improved CMAQ.

Type	Reactions	No.	Comment
Original CMAQ			
Gas-phase chemistry	$\text{OH} + \text{NO}_2 \rightarrow \text{HNO}_3$	R1	
	$\text{N}_2\text{O}_5 + \text{H}_2\text{O} \rightarrow \text{HNO}_3$	R7	
	$\text{HO}_2 + \text{NO}_3 \rightarrow \text{HNO}_3 + \text{OH} + \text{NO}_2$	R8	
	$\text{NO}_3 + \text{VOCs}^a \rightarrow \text{HNO}_3$	R9	
Heterogeneous chemistry	$\text{N}_2\text{O}_5(\text{g}) + \text{H}_2\text{O}(\text{aq}) \rightarrow 2\text{HNO}_3(\text{g})$	R5	
	$\text{NO}_2(\text{g}) + \text{H}_2\text{O}(\text{aq}) \rightarrow \text{HONO}(\text{g}) + \text{HNO}_3(\text{g})$	R10	
Improved CMAQ			
Newly added or revised heterogeneous reactions	$\text{N}_2\text{O}_5(\text{g}) + \text{H}_2\text{O}(\text{aq}) + \text{Cl}^-(\text{aq}) \rightarrow \text{ClNO}_2 + \text{NO}_3^-(\text{aq})$	R6	Revise R5
	$2\text{NO}_2(\text{g}) + \text{Cl}^-(\text{aq}) \rightarrow \text{ClNO}(\text{g}) + \text{NO}_3^-(\text{aq})$	R11	Revise R10
	$\text{NO}_3 + 2\text{Cl}^-(\text{aq}) \rightarrow \text{Cl}_2(\text{g}) + \text{NO}_3^-(\text{aq})$	R12	Increase $\text{NO}_3^-$
	$2\text{Cl}^-(\text{aq}) + \text{O}_3(\text{g}) + \text{H}_2\text{O}(\text{aq}) \rightarrow \text{Cl}_2(\text{g}) + 2\text{OH}^-(\text{aq}) + \text{O}_2(\text{g})$	R13	Affect OH
	$\text{OH}(\text{g}) + \text{Cl}^-(\text{aq}) \rightarrow \text{Cl}_2(\text{g}) + 2\text{OH}^-(\text{aq})$	R14	Affect OH
	$\text{ClONO}_2(\text{g}) + \text{Cl}^-(\text{aq}) + \text{H}^+(\text{aq}) \rightarrow \text{Cl}_2(\text{g}) + \text{HNO}_3(\text{g})$	R15	Affect OH
	$\text{HOCl}(\text{g}) + \text{Cl}^-(\text{aq}) + \text{H}^+(\text{aq}) \rightarrow \text{Cl}_2(\text{g}) + \text{H}_2\text{O}(\text{aq})$	R16	Affect OH
	$\text{ClNO}_2(\text{g}) + \text{Cl}^-(\text{aq}) + \text{H}^+(\text{aq}) \rightarrow \text{Cl}_2(\text{g}) + \text{HONO}(\text{aq})$ (PH < 2.0)	R17	Affect OH
$\text{ClNO}_2(\text{g}) \rightarrow \text{Cl}^- + \text{NO}_3^- + 2\text{H}^+$ (pH ≥ 2.0)	R18	Increase $\text{NO}_3^-$	

566 <sup>a</sup>: presents different VOCs species. In SAPRC 11 mechanism, the VOCs species include CCHO  
 567 (Acetaldehyde), RCHO (Lumped C3+ Aldehydes), GLY (Glyoxal), MGLY (Methyl Glyoxal),  
 568 PHEN (phenols), BALD (Aromatic aldehydes), MACR (Methacrolein), IPRD (Lumped isoprene  
 569 product species).  
 570



571 Table 3 The uptake coefficient of  $N_2O_5$  in different Scenarios and its impact on nitrate (unit:  $\mu\text{g m}^{-3}$ )  
572 <sup>3)</sup> (uptake coefficient of  $N_2O_5$  detrivies from Bertram et al. (Scenario1), Davie et al.(Scenario2), and  
573 Zhou et al.(2018), repectively)

	Obs	Scenario1		Scenario2		Scenario3	
		$\gamma_{N_2O_5}$	$NO_3^-$	$\gamma_{N_2O_5}$	$NO_3^-$	$\gamma_{N_2O_5}$	$NO_3^-$
06/11-D	2.54	0.033	1.59	0.008	1.32	0.09	2.17
06/11-12-N	2.42	0.043	1.67	0.037	1.37	0.09	2.12
06/12-D	3.39	0.028	2.16	0.032	2.74	0.09	3.13
06/12-13-N	4.24	0.021	4.02	0.022	4.05	0.09	6.04
06/13-D	2.57	0.012	1.18	0.008	1.06	0.09	2.47
06/13-14-N	4.10	0.022	4.45	0.022	4.45	0.09	7.13
06/14-D	0.95	0.001	1.34	0.001	1.33	0.09	1.64
06/14-15-N	2.75	0.013	1.00	0.007	0.96	0.09	2.33
06/15-D	0.75	0.001	0.66	0.001	0.66	0.09	1.11

574